



Improvement of FEA estimations for compression behavior of Mg foams based on experimental observations



J.H. Cadena^a, I. Alfonso^{a,*}, J.H. Ramírez^b, V. Rodríguez-Iglesias^b, I.A. Figueroa^a, C. Aguilar^c

^a Instituto de Investigaciones en Materiales, Universidad Nacional Autónoma de México, Circuito Exterior SN, Cd. Universitaria, Del. Coyoacán, México D.F. C. P. 04510, Mexico

^b Facultad de Ingeniería, Universidad Autónoma del Carmen, Campus III, Avenida Central S/N, Esq. con Fracc. Mundo Maya, Ciudad del Carmen, Campeche C. P. 24115, Mexico

^c Departamento de Ingeniería Metalúrgica y Materiales, Universidad Técnica Federico Santa María, Av. España 1680, Casilla 110-V, Valparaíso, Chile

ARTICLE INFO

Article history:

Received 6 February 2014

Received in revised form 25 April 2014

Accepted 29 April 2014

Available online 24 May 2014

Keywords:

Foam

Mg

FEA

Simulation

Compression

ABSTRACT

This work reports the comparative compression behavior between Finite Element Analysis (FEA) estimations and experimental results, for Mg foams with regular pore size and porosities ranging from 25% to 45%, obtained by means of powder metallurgy. Results showed an important decrease in the Young's modulus as the porosity increases for both, the experimental results and FEA estimations. Due to the presence of interconnected pores and additional porosity for the manufactured foams, a correction equation was introduced to the predictions to avoid mismatched results originated from the differences between the foams and the FEA models. Estimations obtained using this equation were in good agreement with the experimental results, showing that the use of FEA is an interesting tool for predicting the mechanical properties of metallic foams before the design and fabrication, even when the modeled pore network presents important differences compared to the foam experimentally produced.

© 2014 Elsevier B.V. All rights reserved.

1. Introduction

In the last two decades metallic foams have been developed for use as new functional materials, since these materials present a unique combination of physical and chemical properties derived from their structure [1]. Metallic foams show increasing potential for applications in a wide range of structural and functional products, due to their exceptional mechanical, thermal, acoustic, electrical and chemical properties [2–4]. These materials can be manufactured by a wide variety of methods, including processes with the metal in solid, liquid and gaseous states. Commonly used methods based on the solid and liquid states involve the incorporation of a removable space holder phase. Two of the most important methods are the infiltration of liquid metal and conventional powder metallurgy (PM) [5,6]. Zhao and Sun [7] developed a technique for manufacturing open-cell foams at low cost using the PM route, known as the Sintering and Dissolution Process (SDP). The SDP has been used to date to obtain mainly aluminum (Al) foams, which show good properties and interconnected pores. It is worth noting that, at present, and due to the difficulty of working with Mg powders (such as their pyrophoric nature when small), only a few papers have reported the successful production of Mg foams

through such methods [8,9]. It is very important to have predictions of the foam mechanical behavior before their fabrication in order to optimize the design process depending on the desired properties and applications. The importance of these predictions is high for the analysis of new products, like Mg foams obtained by SDP. One of the methods used to predict foams properties is the Finite Elements Analysis (FEA), also used for the study of nano-structured materials, composites, granular materials, etc. FEA is very useful to analyze foams due to its modeling capability, being able to model different geometries and analyze their effect on the mechanical properties. Different reports [10–13] have used a wide variety of pore models for the analysis of the foams, mainly to study the compressive mechanical properties, showing that almost all models and simulations over-predict the foam strength for connected or interconnected pores. For foam models based on finite element analysis, the validity of the predictions depends on the proximity of the model to the real foam topology. This fact has led to investigate new models and modifications, in order to obtain results in better agreement with the experimental results than those obtained using conventional models. These new models have a good potential for designing and developing foams for practical engineering parts. In the present work, the SDP route is employed to obtain magnesium (Mg) foams with regular pore size using Mg powders and space holder diameter sizes much larger than those reported in the literature. It is important to predict the foams behavior before their manufacture, in order to obtain a better

* Corresponding author. Tel.: +52 5556223857.

E-mail address: ialfonso@unam.mx (I. Alfonso).

approach to the microstructure and a good correlation porosity-properties. Based on the above, the objective of the present work is to analyze by FEA the effect of the porosity on the compressive behavior of Mg foams. The comparison of the obtained predictions with the experimental results for foams produced by the SDP route and the introduction of a correcting equation in order to obtain more accurate results will also be assessed.

2. Experiment and calculation

The FEA models used in this work for the analysis of Mg foams were led by the necessity of comparing the estimations and experimental results. Before the selection of the Mg foam models, in order to obtain a better prediction of the real microstructures, it is important to know about the characteristics of the manufacturing process. This process consisted on obtaining Mg foams with different porosities by means of powder metallurgy with a space holder. The metal powder used for processing the foams was Mg (99.5% purity, Alfa Aesar) with diameters ranging from 400 μm to 500 μm . Spherical carbamide ($\text{CH}_4\text{N}_2\text{O}$) granules (99% purity, Sigma Aldrich) with diameters in the range from 1 mm to 2 mm were selected as the Space Holder Particles (SHP). With the aim of ensuring good adhesion of Mg powders, ethanol 2 vol.% was sprayed on carbamide particles before the mixing stage to obtain a sticky surface. Then, the mixture was introduced into a steel mold and uniaxially pressed to produce cylindrical compacts with 13.0 ± 1.0 mm in diameter and 15.0 ± 1.0 mm in length. The pressure used for the compaction stage was 300 MPa for all samples. The carbamide fraction of the green compact formed at this stage was dissolved by immersion in a water bath at 25 $^\circ\text{C}$ for 1 h, revealing the spherical pores. Finally, the sintering process was carried out at 620 $^\circ\text{C}$ under an Ar atmosphere. The microstructures of the obtained foams were characterized by Scanning Electron Microscopy (Jeol JSM 7600F, operated at 20 keV) to determinate the pore size, the quality of the metallurgical bond between the metallic powders and the interconnection of the pores. The Young's moduli of the specimens, measured by means of compression tests, were conducted on an Instron 1125-5500R materials testing machine with a crosshead speed of 0.1 mm/min, according to the ASTM E9-09. The porosities of the foams were designed to be 25%, 35% and 45%, obtained mixing Mg and carbamide in proportions of 80–20, 70–30 and 60–40 (in wt.%), respectively. The real foam porosity, P_f , was determined through the following equation [7]:

$$P_f = (1 - \rho_f) / \rho_{Mg} \quad (1)$$

where, ρ_{Mg} is the Mg density and ρ_f is the foam density. Carbamide and Mg densities are 1.34 and 1.74 g/cm^3 , respectively. The densities of the foams were determined using the conventional equation for density, while the volumes were measured by the Archimedes principle.

In order to generate FEA models that simulate the specimens used for the compression tests, the above manufacturing process was taken into account, and the models consisted on cylindrical specimens of 13 mm in diameter and 15 mm in length, with porosities of 25%, 35% and 45%. ANSYS 14.5 FEA software was employed for modeling and theoretical calculations. It is worth noting that the FEA model included spherical pores of 1.5 mm in diameter and homogeneously distributed as per the sample experimental condition. For the case of 45%, the model presented interconnected pores along the x - y plane. The quantity of pores and the distance between them were determined according to the desired total porosity. Fig. 1a–c shows the modeled cylindrical foams with porosities from 25% to 45%.

The Young's moduli of the metallic foams with different porosities were uni-axially estimated when applying equivalent

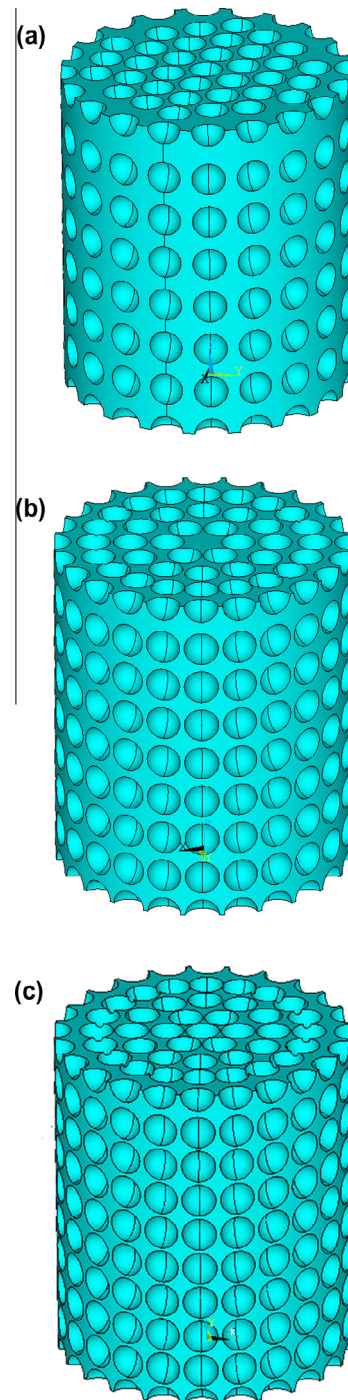


Fig. 1. Finite element models using ANSYS, for the Mg foams with porosities of (a) 25%, (b) 35% and (c) 45%.

compressive stresses on the upper end nodes of the cylindrical specimens. The simulated linearly elastic mechanical compressive testing was compared to experimental measurements. The SOLID187 3-D 10-node tetrahedral structural solid element was employed for meshing with an element size of 0.00025 mm. This element is well suited to modeling irregular meshes, such as those produced for porous materials. The coupled-node boundary condition (keeping the nodes in the same plane) was used for the upper face of the cylinder. This condition is applied, since the presence of pores particles provokes un-even surfaces, and therefore, the deformation measurement was difficult to define. Young's modulus can be

obtained from the response of the compression test, and along the z-axis (E_z) it can be determined by:

$$E_z = \frac{\sigma_z}{\varepsilon_z} \quad (2)$$

where σ_z and ε_z are the stress and the strain in z-axis, respectively. The displacement of the cylinder in z-axis (u_z) is measured from the FEA estimations, and used for the strain determination:

$$\varepsilon_z = \frac{u_z}{L_z} \quad (3)$$

where L_z is the original height of the cylindrical specimen. The Young's modulus (1.5 GPa) and Poisson's Ratio (0.29) used for simulations were obtained from the results of the compressive test of a specimen sintered without space holder particles.

3. Results and discussion

Fig. 2a–c shows SEM micrographs of the experimentally obtained foams with different porosities. As it can be observed, the foams present pores not only produced by the SHP (both connected and not connected pores) but also additional porosity associated to the sintering process of Mg particles (interparticle porosity). These additional pores increase the total porosity values of the foams. The regions enclosed by the black circles display the approximate dimensions of the spherical carbamide employed to produce the foams, matching with the pores size. Fig. 2a (80% Mg – 20% carbamide) and b (70% Mg – 30% carbamide) show separated cells with low pore interconnectivity, while Fig. 2c (60% Mg – 40% carbamide) shows a significant increase in pores interconnectivity. These results show that the modeled porosities are mismatched to the experimental results, fact that this could significantly modify the predictions obtained by the FEA models. The real porosities of the experimentally produced foams (obtained using Eq. (1)) were 31%, 42% and 51%, while their densities were 1.18, 1.07 and 0.94 g/cm³, respectively.

The graphical response of the models to the distributed applied loads for the foams with different porosities can be observed in Fig. 3a–c. This figure shows that total displacement is directly proportional to the porosity. Maxima displacements from the initial size increased from 1% to 1.7% when the porosity increased from 25% to 45%. These results were used to determine Young's moduli (Eqs. (2) and (3)).

The FEA estimated results and experimental values for the Young's moduli are compared in Table 1. The results for the specimen sintered without SHP are also shown. As observed, the Young's moduli significantly decreases when porosity increases in a similar way for both, predictions and experimental values. The Young's modulus for the experimental foam with a porosity of 25% is 0.79 GPa, decreased down to 0.29 GPa for the foam with a porosity of 45%. For the specimen without induced porosity (Mg particles without SHP), the estimation and experimental value were found to be very close, i.e. 1.57 and 1.50 GPa, respectively. The resulting small relative error (4.38%) could be attributed to the fact that the modeled topology is close to the real one, with no additional pores. Because of the presence of the above-mentioned additional pores, the relative errors between estimations and experimental values significantly increased for the foams with higher porosities. The maximum relative error (105.17%) was obtained for the foam with the highest porosity, showing that the selected models were not accurate enough, as the experimental porosities were slightly higher than the expected (modeled).

After the comparative analysis of the results obtained so far, a correction equation that minimizes the errors due to the presence of porosity higher than modeled was introduced. The proposed equation for correcting the estimated Young's modulus (E_f) is

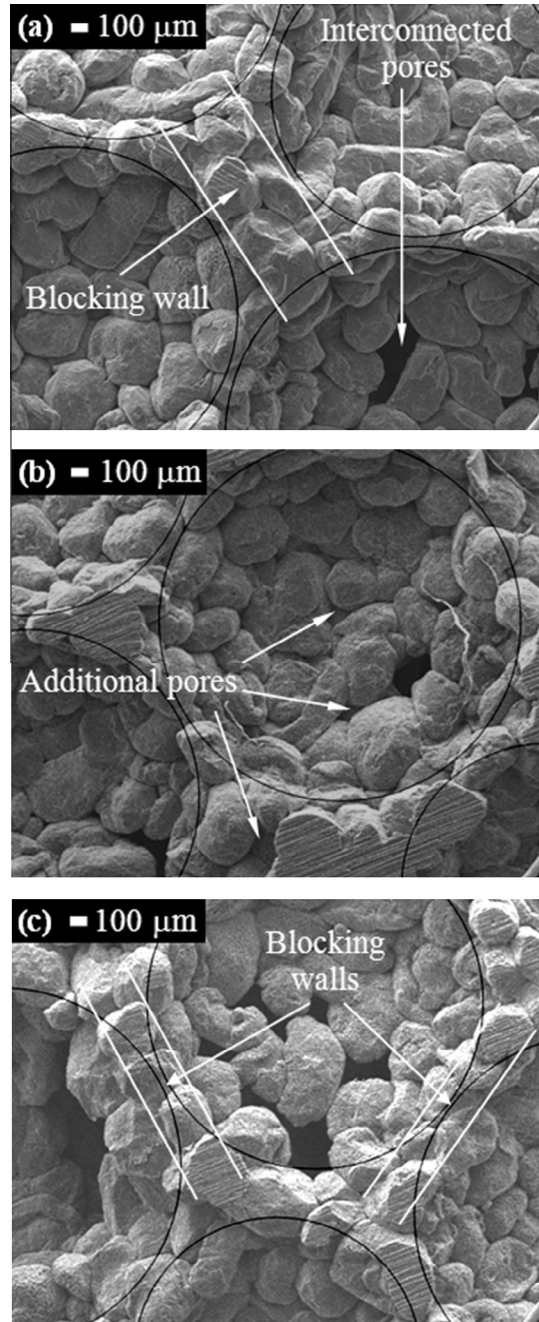


Fig. 2. Scanning Electron Microscopy images of the metallic foams obtained using different Mg- carbamide proportions (a) 80–20%, (b) 70–30% and (c) 60–40%.

shown below. This includes the Young's modulus estimated using FEA, and is dependent of the modeled porosity:

$$E_f = E_s \left(\frac{e}{\phi} \right)^{1/2} \quad (4)$$

where E_s is the Young's modulus estimated using FEA, e is the relative error between modeled and real porosities, and ϕ is the porosity used in the FEA model. This equation was obtained using the trial and error method, taken into account that we observed that for all the studied foams the ratio between modeled and real porosities remained almost constant (0.8, approximately), decreasing their relative errors (e) when the porosity (ϕ) increased. We also observed that relative errors for the Young's moduli estimated using FEA significantly increased for high porosities. That is why we

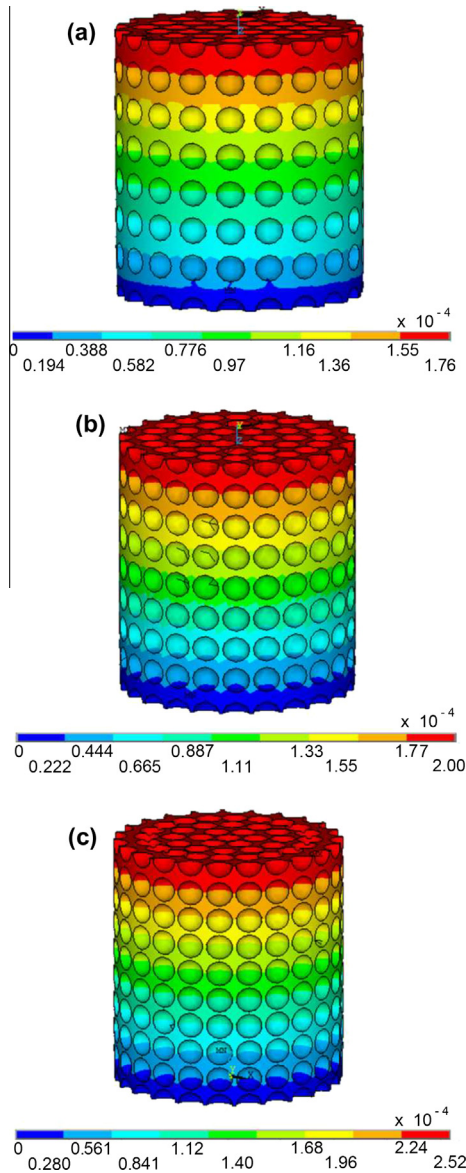


Fig. 3. Deformation (in m) of the Mg foam models under compression, with porosities of (a) 25%, (b) 35% and (c) 45%.

Table 1
Estimated and experimental Young's moduli (in GPa) for the materials with different porosities.

	Foam porosity (%)			
	0 (without SHP)	25	35	45
E, FEA estimated	1.57	0.86	0.72	0.59
E, experimental	1.50	0.79	0.45	0.29
Relative error (%)	4.38	8.48	60.00	105.17

included these two parameters (e and ϕ) in the equation, and searched for a correction factor that matched estimated and experimental Young's moduli (this factor is the square root). With this formula, it was possible to significantly decrease the differences between the estimated and experimental values, as observed in Table 2. The highest resulting relative error using this correction was 10.41%, which is much smaller than obtained using only FEA estimations, showing that the effect of the additional porosity was drastically minimized. Future works will be focused on refining

Table 2
Corrected FEA and experimental Young's moduli (in GPa) for the foams with different porosities.

	Foam porosity (%)		
	25	35	45
E, FEA corrected	0.76	0.50	0.30
E, experimental	0.79	0.45	0.29
Relative error (%)	4.22	10.41	4.59

Table 3
Young's moduli (in GPa) obtained using different models and experimental results for the foams with different porosities.

	Foam porosity (%)		
	25	35	45
E, experimental	0.79	0.45	0.29
E, Zhu	0.76	0.66	0.55
Relative error (%)	4.27	46.97	90.31
E, experimental	0.79	0.45	0.29
Warren–Kraynik	0.63	0.55	0.46
Relative error (%)	20.31	22.12	58.08

the porosity model depending on the Mg/SHP proportions, the size of the Mg particles and the pressure used for the compaction stage.

In order to compare the effectiveness of our FEA corrected predictions, two reported models for calculating elastic modulus were used. The first was the model obtained by Zhu et al. [14]:

$$E_f = \frac{1.009E_s\rho^2}{1 + 1.514\rho} \quad (5)$$

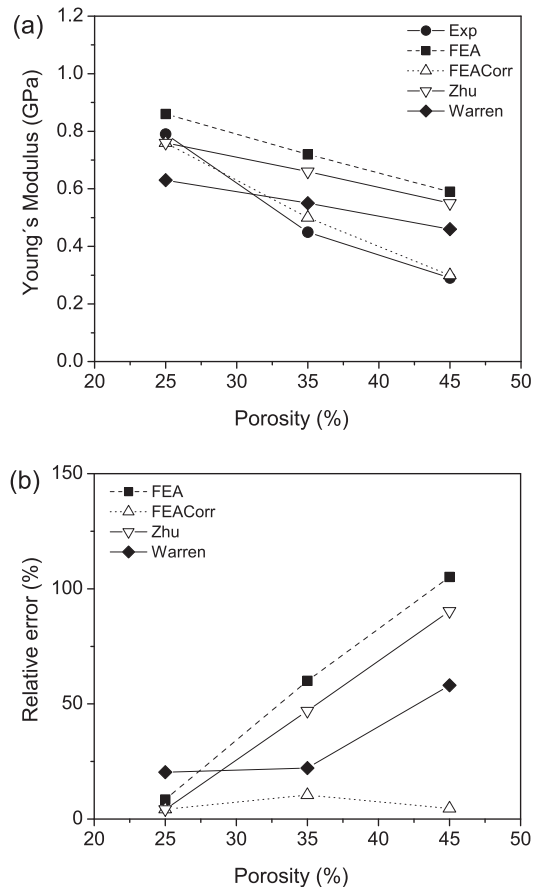


Fig. 4. (a) Compressive Young's modulus variation with porosity, and (b) their errors.

where E_s is the Young's modulus of the solid material and ρ is the relative density of the foam. The second model is the study by Warren and Kraynik [15], where:

$$E_f = \frac{E_s \rho^2 (11 + 4\rho)}{(10 + 31\rho + 4\rho^2)} \quad (6)$$

The estimations obtained using these models are listed in Table 3. As it can be observed, relative errors are rather high, especially at low densities, where high porosities and different topologies of the foams provoked important mismatches between experimental results and estimations, overpredicting the foam strength.

For a complete analysis of the results of the present work for Mg foams, Fig. 4a and b shows the Young's modulus variation vs porosity, and the relative errors of these values as a function of the experimental results. It can be clearly observed that the FEA corrected model estimations are very close to the experimental results, obtaining the lowest errors. These results show the importance of FEA for the study of foams, predicting in a rather accurate way their compressive behavior. The FEA modeling capability allowed to take into account not only the constituent material properties and the porosity percentage, but also the size and shape of the pores, and the strength of the bonding between the grains in the sintering process. This helped to obtain predictions closer to the experimental results than the models that only include the porosity or the density of the foams. The selection of the foam topology has demonstrated to be an essential variable for obtaining a correct estimation.

4. Conclusions

In this work, three-dimensional models were used in order to predict the compressive behavior of Mg foams with porosities of 25%, 35% and 45%. Results showed that the porosities obtained for the experimental foams are significantly higher than expected/ modeled. This was provoked by the presence of interconnected pores and additional pores in the spaces between individual Mg particles. The estimated and experimental Young's moduli significantly decreased with porosity in a similar way. Nevertheless,

relative errors between estimations and experimental values were very high for the foams with high porosities. The introduction of a correction equation to the FEA predictions made possible an important decrease in the differences between the estimated and experimental values. Finally, the comparisons with the reported foam models showed that proposed FEA model predicted more accurately the compressive behavior of the experimentally produced foams.

Acknowledgements

The authors would like to acknowledge the financial support from SENER-CONACYT 151496 and UNAM PAPIIT TA100114 for funding the project. A. Tejada-Cruz, E. Ortiz, G.A. Lara-Rodríguez, J.J. Camacho, J. Morales-Rosales, C. Delgado, S. Báez, O. Novelo-Peralta, C. González and E. Sanchez are also acknowledged for their technical support.

References

- [1] G.J. Davies, S. Zhen, *J. Mater. Sci.* 18 (1983) 1899.
- [2] L.J. Gibson, M.F. Ashby, *Cellular Solids: Structure and Properties*, 2nd ed., Cambridge University Press, Cambridge UK, 1997.
- [3] J. Banhart, H. Eifert, *Metal Foams*, Verlag MIT Publishing, Bremen, 1997.
- [4] J. Banhart, M.F. Ashby, N.A. Fleck, *Metal Foams and Porous Metal Structures*, Verlag MIT Publishing, Bremen, 1997.
- [5] M.F. Ashby, A.G. Evans, N.A. Fleck, L.J. Gibson, J.W. Hutchinson, H.N.G. Wadley, *Metal Foams: A Design Guide*, Butterworth-Heinemann, USA, 2000.
- [6] J. Banhart, *Prog. Mater. Sci.* 46 (2001) 559.
- [7] Y.Y. Zhao, D.X. Sun, *Scr. Mater.* 144 (2000) 105.
- [8] C.E. Wen, Y. Yamada, K. Shimojima, Y. Chino, H. Hosokawa, M. Mabuchi, *Mater. Lett.* 58 (2004) 357.
- [9] C.E. Wen, M. Mabuchi, Y. Yamada, K. Shimojima, Y. Chino, T. Asahina, *Scr. Mater.* 45 (2001) 1147.
- [10] S. Kari, H. Berger, U. Gabbert, R. Guinovart-Díaz, J. Bravo-Castillero, R. Rodríguez-Ramos, *Compos. Sci. Technol.* 68 (2008) 684–691.
- [11] A. Hasan, An improved model for FE modeling and simulation of closed cell Al-alloy foams, *Adv. Mater. Sci. Eng.* 2010 (2010) 12.
- [12] K.M. Ryu, J.Y. An, W.S. Cho, Y.C. Yoo, H.S. Kim, *Mater. Trans.* 46 (2005) 622–625.
- [13] M. Kirca, A. Gul, E. Ekinci, F. Yardim, A. Mugan, *Finite Elem. Anal. Des.* 44 (2007) 45–52.
- [14] H.X. Zhu, N.J. Mills, J.F. Knott, *J. Mech. Phys. Solids* 45 (1997) 1875–1904.
- [15] W.E. Warren, A.M. Kraynik, *ASME J. Appl. Mech.* 55 (1988) 341–346.